AD-A214 551

DTIC ELECTE NOV 17 1989 S B D

DOCUMENTATION PAGE

Form Approved OMB No 0704-0188

1a REPORT SECURITY CLASSIFICATION: (U)	1b RESTRICTIVE MARKINGS: NA
2a SECURITY CLASSIFICATION AUTHORITY: NA	3 DISTRIBUTION / AVAILABILITY OF REPORT: Distribution Unlimited
2b DECLASSIFICATION / DOWNGRADING SCHEDULE: NA	
4 PERFORMING ORGANIZATION REPORT NUMBER(S): University of North Carolina at Chapel Hill	5 MONITORING ORGANIZATION REPORT NUMBER(S): NA
6a NAME OF PERFORMING ORGANIZATION: University of North Carolina at Chapel Hill	6b OFFICE SYMBOL (If applicable): NA
6c ADDRESS (City, State, and ZIP Code): Department of Cell Biology & Anatomy, CB# 7090, 236 Taylor Hall, Chapel Hill, NC 27599-7090	7a NAME OF MONITORING ORGANIZATION: Office of Naval Research
	7b ADDRESS (City, State, and ZIP Code): 800 N. Quincy Street, Arlington, VA 22217-500C
8a NAME OF FUNDING / SPONSORING ORGANIZATION: Office of Naval Research	8b OFFICE SYMBOL (If applicable):
	9 PROCUREMENT INSTRUMENT IDENTIFICATION NUMBER: N00014-89-J-1433
8c ADDRESS (City, State, and ZIP Code): 800 N. Quincy Street, Arlington, VA 22217-5000	10 SOURCE OF FUNDING NUMBERS: PROGRAM ELEMENT NO. 61153N; PROJECT NO. RR04108; TASK NO. 441Q908; WORK UNIT ACCESSION NO.
11 TITLE (Include Security Classification): (U) Rescue of Injured Myocytes	
12 PERSONAL AUTHOR(S): Lemasters, John J.	
13a TYPE OF REPORT: Annual	13b TIME COVERED: FROM 12/88 TO 12/89
14 DATE OF REPORT (Year, Month, Day):	15 PAGE COUNT:
16 SUPPLEMENTARY NOTATION:	

17 COSATI CODES			18 SUBJECT TERMS (Continue on reverse if necessary and identify by block number)
FIELD	GROUP	SUB-GROUP	
08			

19 ABSTRACT (Continue on reverse if necessary and identify by block number)

The critical events leading in to the transition from reversible to irreversible hypoxic and toxic injury to cells remain poorly understood. In recent studies, we have measured changes in cytosolic free Ca^{2+}, mitochondrial membrane potential, cytosolic pH, cell surface blebbing and other factors in relation to the onset of cell death following anoxic and toxic injury to single hepatocytes and myocytes. The major technical approach we have taken for this work utilizes Multiparameter Digitized Video Microscopy (MDVM). In MDVM, living cells are labeled with multiple fluorescent probes. Each probe responds to a defined cellular parameter by emitting fluorescent of a specific wavelength. MDVM permits florescence of each probe to be sampled, quantified and

20 DISTRIBUTION / AVAILABILITY OF ABSTRACT: ☒ UNCLASSIFIED/UNLIMITED ☐ SAME AS RPT ☐ DTIC USERS	21 ABSTRACT SECURITY CLASSIFICATION: (U)
22a NAME OF RESPONSIBLE INDIVIDUAL: Dr. J.A. Majde	22b TELEPHONE (Include Area Code): 202/696-4055 — 22c OFFICE SYMBOL: ONR

DD Form 1473, JUN 86 — Previous editions are obsolete. — SECURITY CLASSIFICATION OF THIS PAGE

DISTRIBUTION STATEMENT A
Approved for public release;
Distribution Unlimited

S/N 0102-LF-014-6603

89 11 16 126

Section 1. Overview of Progress: MULTIPARAMETER DIGITIZED VIDEO MICROSCOPY (MDVM) OF HYPOXIC CELL INJURY (with A.-L. Nieminen, T.L. Dawson, B.E. Wray, T. Kawanishi, Y. Tanaka, K. Florine-Casteel, J.M. Bond and B. Herman)

INTRODUCTION

Cell death from disease is rarely synchronous, and events leading to irreversible injury may be obscured when large cell populations are studied, especially if these events occur rapidly or suddenly. To overcome this drawback, we have made measurements of single living cells during hypoxic and toxic stress using a rapidly developing technology called multiparameter digitized video microscopy (MDVM). Beginning in 1985, we have monitored on a quantitative basis numerous cell parameters, including cytosolic free Ca^{2+}, mitochondrial membrane potential, cytoplasmic pH, plasma membrane permeability, cell surface morphology and cell viability. By comparing the time courses of changes of individual parameters, new insight has been obtained into the mechanisms of anoxic, hypoxic and toxic injury in single living cells.

MDVM SYSTEM

The basic components of our MDVM system are an inverted microscope, an intensified silicon-intensified target (ISIT) video camera, and a computer equipped with analog-to-digital converters and frame memories for image processing and analysis (Figure 1) (see also DiGuiseppi et al., 1985; Gores et al., 1989a). The high sensitivity of the ISIT camera together with the frame averaging capability of the computer allows us to work at very low levels of excitation energy and fluorophore concentrations, thus preventing photobleaching and photodamage which might disrupt cell function. The ISIT camera can also be used to obtain bright field images allowing acquisition of phase contrast and fluorescent images from the same cells. In a typical experiment, we record phase contrast images continuously at low illumination using a video casette recorder with brief interruptions to collect digitized fluorescent images. Phase contrast images show us changes in cell structure which are then correlated with quantitative changes in fluorescent images. These MDVM determinations are further correlated with electron microscopy, bulk biochemical determinations, measurements of cell volume, and other assays.

In order to sample the fluorescence of several different fluorophores during a single experiment, specimens must be illuminated at various different wavelengths and fluorescence of various colors imaged through the microscope. To facilitate selection of excitation and emission wavelengths, we have constructed computer-driven excitation and emission filter changers for programmable, automated operation. The excitation filter changer consists of a pair of 10-place filter

wheels. One wheel contains interference filters for wavelength selection. The other wheel contains neutral density filters to control the intensity of illumination. The emission filter changer holds 4 dichroic mirror/barrier filter assemblies and is used to select the emission wavelength.

FLUORESCENT PROBES OF CELLULAR FUNCTIONS

The experimental approach we follow takes advantage of a number of different fluorescent compounds whose excitation and emission spectra are sensitive to specific environmental parameters and which preferentially accumulate into specific subcellular compartments of living cells (Table 1) (see also Tsien, 1989; Haugland, 1989). This enables us to study multiple cellular functions in individual cells in response to external stimuli, and we have shown that four or more variables can be monitored in the same living cell by selecting parameter-specific fluorophores with non-overlapping emission and excitation spectra. We are fortunate that the number of parameter-sensitive probes available is large and constantly expanding. For the studies reviewed here, we used Fura-2 to measure cytosolic free Ca^{2+} (Grynkiewicz et al., 1985), rhodamine 123 to monitor mitochondrial membrane potential (Johnson et al., 1981; Emaus et al., 1986), BCECF (2',7'-biscarboxyethyl-5,6-carboxyfluorescein) to measure cytosolic pH (Bright et al., 1987), and propidium iodide to label the nuclei of nonviable cells (Lemasters et al., 1987).

RATIO IMAGING

Quantitative MDVM provides information regarding the spatial and temporal characteristics of fluorophore emission. However, the strength of emission will not only be proportional to the environmental parameter of interest but also to regional variations of cell thickness and fluorophore concentration. To offset these variations, images can be acquired from cells at two different excitation wavelengths, one which is parameter-sensitive and one which is not. By dividing (ratioing) these images, errors introduced by differences in cell thickness and fluorophore concentration are corrected. Such ratio-imaging is used with Fura-2 to determine cytosolic free Ca^{2+} and with BCECF to determine cytosolic pH.

EXPERIMENTAL MODELS OF HYPOXIC CELL INJURY

We use two basic protocols to produce or simulate hypoxic injury in cultured rat hepatocytes. True anoxia is established by perfusing an environmental chamber mounted on the video microscope with submitochondrial particles (Herman et al., 1988). In the presence of an oxidizable substrate such as succinate, the submitochondrial particles actively consume oxygen and reduce pO_2 to less than 1 torr with 2-3 minutes.

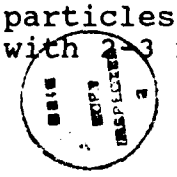

Another model employs KCN and iodoacetate (or 2-deoxyglucose) to inhibit ATP production by oxidative phosphorylation and glycolysis (Lemasters et al., 1987). This treatment, called 'chemical hypoxia', mimics the ATP depletion and reductive stress that accompanies anoxia. Our studies have shown that the two models are comparable in many, although not all respects. We use the model of chemical hypoxia principally because it is less demanding technically. Certain experiments such as measurements of cell volume with a Coulter counter are simply impossible to perform under conditions of true anoxia.

ANOXIC AND HYPOXIC INJURY

Cell Surface Blebbing and Cell Death

Bleb formation similar to that observed in intact liver during hypoxia (Lemasters et al., 1981, 1983) occurs in both models of hypoxic cell injury (Lemasters et al., 1987; Herman et al., 1988; Nieminen et al., 1988). Three stages can be recognized. Stage I is characterized by formation of numerous small blebs on cell surfaces. During Stage II, blebs grow and coalesce by fusion until 1-3 large terminal blebs remain. Bleb fusion is extremely rapid and occurs faster than the video frame rate (33 msec). Stage III is initiated by outright rupture of one of the terminal blebs and is followed by loss of trapped cytosolic markers (e.g., Fura-2, BCECF) and uptake of external dyes (e.g., propidium iodide, trypan blue) (Figure 2). The time required for progression of cells through Stages I-III varies from cell to cell. For chemical hypoxia, progression to cell death takes place after as little as 30 minutes or as long as 90 minutes. Thus, observation of bleb formation in single cells in relation to other cellular parameters is essential to reach meaningful conclusions regarding mechanisms of lethal cell injury.

Changes of the structural integrity of the plasma membrane appear after bleb lysis. In Figure 2A, a field of two cells is imaged by video microscopy after about 65 minutes of chemical hypoxia. These cells have progressed into Stage II of injury. After a bleb on one of the cells ruptures (Figure 2B), propidium iodide is taken up by that cell (Figure 2C). Seconds later the cells were fixed. Scanning electron microscopy of the cell not taking up propidium iodide reveals a continuous cell surface with large intact blebs (Figure 2D). In the cell taking up propidium iodide, a discontinuity in the membrane surface is seen which is rimmed by vesiculated fragments of membrane. Thus, bleb rupture causes a discontinuity to form in the plasma membrane. The abrupt formation of this plasma membrane defect appears to be the cellular basis for the onset of cell death. Recent evidence also suggests that the lipids of blebbed membranes at first become more fluid. Subsequently, blebs become more rigid or gel-like prior to membrane lysis and cell death (Florine-Casteel et al., 1989)

Transition from Reversible to Irreversible Injury

Bleb rupture precipitates cell death, but irreversible injury (i.e., an injury from which the cell cannot recover) may occur earlier. Therefore, we reoxygenated anoxic hepatocytes to determine at what point the injury is no longer reversible (Herman et al., 1988). Anoxia inside a gas-tight chamber mounted on the microscope was achieved using submitochondrial particles. Reoxygenation was induced by washing out the submitochondrial particles with fresh, oxygenated medium. When cells in Stages I and II of bleb development were reoxygenated, blebs were resorbed within a few minutes. No lethal reoxygenation injury occurred in this interval, and the cultured hepatocytes continued to exclude propidium iodide. However, in cells which had already lost viability by the criterion of propidium iodide staining (Stage III), reoxygenation did not reverse bleb formation or lead to any other change in cell structure. Thus in hepatocytes, the onset of cell death and the transition from reversible to irreversible anoxic injury occurred simultaneously.

Cytosolic Free Ca^{2+} during Cell Injury

A rise of cytosolic free Ca^{2+} is suggested to initiate a series of harmful processes which culminate in cell death (see Bellomo and Orrenius, 1985). Using ratio imaging of Fura-2 fluorescence, we monitored free Ca^{2+} during chemical hypoxia with KCN plus iodoacetate in relation to mitochondrial membrane potential, bleb formation and the onset of cell death (Lemasters et al., 1987; Nieminen et al., 1988). Unexpectedly, chemical hypoxia was not associated with increased cytosolic free Ca^{2+} up to the point of cell death despite the presence of cell surface blebbing (Figure 3). However, in the minute or two preceding labeling by propidium iodide, free Ca^{2+} did increase coincident with leakage of Fura-2 from the cells. This increase occurred in high Ca^{2+} (1.2 mM) but not in low Ca^{2+} ($\approx$2 μM) medium. However, rates of cell killing were identical in low and high Ca^{2+} media (Figure 4). These findings indicate that the increase of free Ca^{2+} just prior to propidium iodide labeling does not contribute to lethal cell injury.

The question remains as to how ATP-depleted hepatocytes can maintain a very large Ca^{2+} gradient across the plasma membrane. One hypothesis is that normal pathways for cytosolic entry of ions including Ca^{2+} are shut down during hypoxia. Jones and coworkers (Andersson et al., 1987; Aw et al., 1987) have described such a phenomenon for mitochondrial membranes during anoxic stress, and a high degree of impermeability of mitochondria to small ions was demonstrated during anoxia to isolated hepatocytes. Hypoxia may cause a similar change of permeability in the plasma membrane. However, preliminary studies with SBFI, a fluorescent probe of cytosolic free Na^+ (Harootunian et al., 1988), indicate that Na^+ enters cultured hepatocytes relatively rapidly during chemical hypoxia. Available evidence suggests that a more specific inhibition of Ca^{2+} entry and release from intracellular stores occurs

during hypoxic stress. Recent experiments show that chemical hypoxia rapidly inhibits oscillations of free Ca^{2+} induced by the Ca^{2+}-mobilizing hormone agonists, phenylephrine and vasopressin.

Mitochondrial Membrane Potential during Chemical Hypoxia

In aerobic cells, an electrochemical gradient of protons across the mitochondrial inner membrane comprised largely of a membrane potential drives ATP formation. Following chemical hypoxia, mitochondrial membrane potential as measured by rhodamine 123 fluorescence decreases steadily concomitant with bleb formation (Lemasters et al., 1987). After loss of cell viability, a large final drop of rhodamine 123 fluorescence occurs, and all rhodamine 123 is lost from the cells. Before bleb rupture, mitochondrial potential decreased about -30 mV or 20% of the initial potential of about -160 mV. In consideration that ATP is depleted by more than 95% within 5 minutes, the relatively small drop of mitochondrial membrane potential is unexpected. However, these findings are independently verified by work showing persistence of the mitochondrial membrane potential in hepatocyte suspensions during anoxia (Andersson et al., 1987).

pH_i and Cell Killing

Acidosis is a salient feature of tissue ischemia. To mimic the acidosis of ischemia in our model of chemical hypoxia, we decreased extracellular pH (pH_o) as we added the metabolic inhibitors, KCN and iodoacetate, to hepatocyte suspensions (Gores et al., 1988). At pH 7.4, cell viability decreased to 10% after 120 minutes, whereas at pH_o 5.5 to 7 cell survival was maintained at 65-85%, nearly the same as normoxic cells (Figure 5). During chemical hypoxia under acidotic conditions, a return to pH 7.4 resulted in a rapid acceleration of cell killing -- a 'pH paradox' in analogy to the oxygen, reperfusion and calcium paradoxes which have received much attention in the heart literature. Inhibition of Na^+/H^+ exchange by amiloride or by substitution of choline for Na^+ increased cell survival substantially, whereas promoting exchange of extracellular Cl^- for extracellular HCO_3^- potentiated cell killing. Moreover, monensin, a Na^+/H^+ ionophore which collapses the pH gradient across the plasma membrane, potentiated cell killing at pH_o of 7.4 but not at pH_o of 6.2. A similar protection by acidosis was also observed in anoxic cardiac myocytes (Bond et al., 1989).

To test the hypothesis that protection against lethal cell injury by acidic pH_o is mediated by cytoplasmic acidification, we measured intracellular pH (pH_i) by ratio imaging of BCECF fluorescence using MDVM (Gores et al, 1989a). In normoxic cells, pH_i closely followed changes of pH_o. However after chemical hypoxia at pH_o of 7.4, pH_i decreased by more than a unit within 10 minutes (Figure 6). There was

little spatial heterogeneity of pH_i in either normoxic or hypoxic cells. After 20 to 30 minutes, pH_i began to rise, BCECF began to leak rapidly from the cells, and cell death as indicated by propidium iodide nuclear staining ensued within 1-2 minutes At acidic pH_o or when Na^+/H^+ exchange was inhibited with choline, pH_i decreased to a greater extent, and the duration of cell survival was prolonged an additional 20-30 minutes. Monensin prevented this acidotic pH_i from forming and accelerated the onset of cell death. ATP depletion at neutral and acidic pH_o was identical and could not explain prolonged cell survival.

The decrease of pH_i appeared to be the result of H^+ release due to hydrolysis of ATP and other organic phosphates. From measurements of the internal buffering capacity of these cells, we estimated that about half of the drop of pH_i during chemical hypoxia was accounted for by ATP hydrolysis. Acidosis was not the consequence of lactic acid accumulation since glycolysis was inhibited by iodoacetate. Experiments comparing HCO_3^--free and HCO_3^--containing buffers indicated that HCO_3^- exchange also was not important in cellular acidification.

Working Hypothesis for Protection by Acidic pH_i

These results indicate that intracellular acidosis protects against cell death from ATP depletion, a phenomenon which may represent a protective adaptation against ischemic injury. Our working hypothesis is that acidic pH_i suppresses autolytic degradation processes (e.g., proteolysis, phospholipid hydrolysis) which are initiated during ATP depletion (Figure 7). Despite suppression at acidic pH_i, these degradative processes lead eventually to an increase of plasma membrane permeability causing H^+ to leak from the cell and pH_i to rise. A positive feedback loop is thus created which accelerates pH-dependent degradative processes, increases membrane permeability further, and culminates rapidly in cell death. This scenario also explains the pH paradox.

Dissociation of Lethal Cell Injury from Cell Swelling

Bleb growth accelerates and cell volume, judged by cross sectional areas, increases rapidly prior to the lethal injury from anoxia and chemical hypoxia. To test the hypothesis that cell swelling promotes lethal cell injury, we examined the relationship between cell volume measured with a Coulter counter, bleb formation and loss of cell viability (Gores et al., 1989b). In isosmotic medium, cells swelled by about 35% during chemical hypoxia. In hypotonic medium (150-200 mOs), cells swelled by 50%, but rates of cell killing were the same as in isosmotic medium. Sucrose (300 mM) in isotonic medium prevented early cell swelling but actually accelerated cell killing. Bleb formation occurred regardless of buffer tonicity, and osmotic swelling in normoxic cells did not cause blebbing. Taken together, these results in-

dicate that cell swelling is not the driving force for bleb formation nor a factor leading to lethal injury.

Pro-oxidant Contribution to Lethal Cell Injury during Chemical Hypoxia

Mannitol is a hydroxyl radical scavenger which is permeant to hepatocytes. Mannitol (300 mM) added to isotonic medium improves cell survival during chemical hypoxia but did not prevent cell swelling. To test the hypothesis that mannitol was protective because of its antioxidant effects, we evaluated other antioxidants (Gores et al., 1989b). Desferrioxamine and (+)-cyanidanol-3, but not the impermeant enzymes, superoxide dismutase and catalase, also delayed lethal cell injury. Cell killing was also reduced during anoxic as compared to aerobic chemical hypoxia implicating oxygen as the source of a toxic metabolite.

To further characterize the pro-oxidant aspect of chemical hypoxia, we adapted a dichlorofluorescin assay developed for flow cytometry to quantitate intracellular formation of hydroperoxides (Gores et al., 1989b). Hydroperoxide formation increased during aerobic but not anaerobic chemical hypoxia consistent with increased rates of cell killing under aerobic conditions.

CONCLUSIONS

We conclude that multiple mechanisms, including oxygen radical formation, contribute to cell killing during chemical hypoxia. Our findings illustrate that the predominant mechanism responsible for lethal hypoxic injury may depend upon the specific circumstances. However, an increase of cytosolic Ca^{2+} as a 'toxic second messenger' does not appear to be important in the events leading up to lethal hypoxic injury.

In clinical situations, oxygen deprivation may be absolute or relative. In ischemia, anoxia is virtually absolute and cell killing results, perhaps exclusively, from ATP depletion. In contrast, when oxygen deprivation is incomplete or intermittent, toxic oxygen species may aggravate and accelerate lethal injury. The mechanisms of hypoxic cell killing have a strong dependence on pH, and the acidosis which occurs naturally in ischemia provides strong protection against the onset of lethal cell injury. Realization that many modes of injury can operate concurrently during hypoxia may lead to better interventional strategies in hypoxic and ischemic disease.

Section 2. Experiments with Cardiac Myocytes

A. REVERSAL OF HYPERCONTRACTION, PROTECTION BY ACIDIC pH, AND CHANGE OF CYTOSOLIC pH DURING 'CHEMICAL HYPOXIA' AND ANOXIA IN CARDIAC MYOCYTES (with J.M. Bond, G.J. Gores and B. Herman)

INTRODUCTION

During anoxia, cardiac myocytes lose contractility and after longer periods progress to a rounded, hypercontracted state that is contemporaneous with sarcolemmal blebbing. Although these cells may continue to exclude vital dyes such as trypan blue, reoxygenation does not immediately restore contractility or reverse the hypercontracted state. Thus, these cells are considered irreversibly injured by most investigators. However, only short-term recovery has been evaluated, typically after 15 or 30 minutes of reoxygenation. Therefore, one aim of this study was to evaluate long term viability and functional recovery of cultured neonatal cardiac myocytes after hypoxic injury using multiparameter digitized video microscopy (MDVM).

A second objective of this study relates to the tissue acidosis during ischemia that results from lactic acid accumulation and ATP hydrolysis. Previous work in hepatocytes indicated that an acidic extracellular pH protected against loss of viability during ATP depletion in a model of 'chemical hypoxia' with metabolic inhibitors (Gores et al., 1988). Moreover, this protection was mediated through changes of intracellular pH (pH_i) (Gores et al., 1989). Accordingly, we have assessed the effect of acidotic extracellular pH on the rate of anoxic killing of cultured neonatal cardiac myocytes and have also measured pH_i during ATP depletion.

METHODS

Myocyte Isolation and Purification

Myocytes were isolated by enzymatic digestion and purified by flow-elutriation by modification of the procedure of Ulrich et al.(1989). Briefly, 10-20 hearts from 2-3 day old rat neonates were minced in a balanced salt solution (BSS) containing 0.81 mM $MgSO_4$, 117 mM NaCl, 5.3 mM KCl, 3.3 mM Na_2HPO_4, 5.6 mM glucose, 20 mM Hepes, 10 U/ml penicillin, and 10 μg/ml streptomycin at pH 7.5. After washing, the minced tissue was added to 40 ml of BSS containing 10% pancreatin (Gibco Laboratories, Grand Island, NY) and 0.03% collagenase D (Boehringer Mannheim Corp., Indianapolis, IN) and incubated with stirring for 20 minutes at 37°C. After settling, the supernatant was removed and centrifuged for 5 minutes at 400-g to yield isolated cells in a pellet. The pellet was resuspended in culture media consisting of Eagle's MEM with 5% fetal bovine serum, 10% horse serum, 10 U/ml penicillin, and 10 μg/ml streptomycin. This procedure was repeated on tissue settling out

before collection of the supernatant. Resuspended pellets from each digestion were pooled into a 20 ml volume and incubated with 20 U DNAse (Sigma Chemical Co., St. Louis, MO) at 37°C for one hour in a reciprocating water bath.

The myocyte suspension was then filtered through 60 micron nylon mesh in preparation for myocyte purification from fibroblasts and endothelial cells by flow elutriation (Beckman centrifugal elutriator #J2-21M/E, rotor #JL-6B). The myocyte suspension was loaded at 2000 rpm for 10 minutes using Eagle's MEM with 10 U/ml penicillin, 10 μg streptomycin, and 1% BSA as the mobile vehicle. With flow rate held constant (21 ml/min), the rotor speed was decreased sequentially to 1850 rpm, 1580 rpm, and 500 rpm at 10 minute intervals. Myocytes were eluted at 500 rpm and their viability routinely exceeded 90% as measured by trypan blue exclusion.

Myocyte Culture

Purified myocytes used to study recovery from hypercontraction were cultured on 35 mm Falcon plastic culture dishes at a density of 5×10^5. For studies involving the effect of an acidic extracellular pH on the rate of anoxic killing, purified myocytes were plated on to circular 29 mm polystyrene coverslips in 35 mm plastic culture dishes at a density of 10^6 cells/dish. Contamination by fibroblasts and endothelial cells after 5 days was less than 10%. Non-purified myocytes were used to measure intracellular pH and were plated at a density of 5×10^5 on glass coverslips. All cultures were incubated in culture media at 37°C in humidified air/5% carbon dioxide. Myocytes contracted spontaneously in groups of 5-20 after about 3 days. Striations were visible after 5 days at which time cells exhibited vigorous, synchronous contractions with rates exceeding 60 beats/minute.

Models for Chemical Hypoxia and True Anoxia

To assess recovery after hypercontraction, myocytes in sterile culture dishes were mounted on the microscope stage. Metabolic inhibition was accomplished using 2.5 mM NaCN and 20 mM 2-deoxyglucose in culture medium supplemented with 20 mM Hepes to mimic the ATP depletion of anoxia (chemical hypoxia). Reversal of metabolic inhibition was accomplished by washing with fresh culture media. Individual cells were observed by phase contrast with an inverted microscope for 48 hours. Sterile conditions were maintained for the duration of the experiment.

For studies using true anoxia, myocytes cultured on polystyrene coverslips were mounted in a gas-tight chamber on the stage of the microscope. Anoxia was created by injection of 1 mg/ml submitochondrial particles and 5 mM succinate in Krebs-Ringers-Hepes (KRH) buffer into the chamber (Herman et al., 1988). 20 mM 2-deoxyglucose was also added to inhibit glycolysis and further deplete ATP.

Determination of Cell Viability

Viability of myocytes was determined using propidium iodide, a fluorescent dye which binds to nuclear chromatin upon loss of cell viability. Propidium iodide fluorescence was imaged using excitation and emission wavelengths of 515 and 620 nm, respectively (Lemasters et al., 1987). Rates of cell killing were determined by observing propidium iodide labeling of myocyte nuclei over time. Total nuclei were determined at the end of each experiment by addition of 10 μM digitonin to permit staining of all cells.

Cytosolic pH Measurement

Intracellular pH was measured in individual 4-day old cultured non-purified myocytes using the pH sensitive fluorophore, 2',7'-biscarboxyethyl-5,6-carboxyfluorescein (BCECF), essentially as described by Gores et al. (1989a). BCECF (5 μM) was loaded as its acetoxymethyl ester for 30 minutes at 37°C. A ratio value was determined from images at excitation wavelengths of 440 nm (pH-independent) and 490 nm (pH-dependent). Calibration was carried out <u>in situ</u> using 10 μM nigericin.

ATP Measurements

ATP levels were determined after perchloric acid extraction by reverse-phase HPLC as described previously (Gores et al., 1988).

RESULTS

Recovery from Hypercontracture

One aim of this study was to assess the long term functional recovery of myocytes after various periods of chemical hypoxia, a model of ATP depletion using inhibitors of oxidative phosphorylation and glycolysis which mimics the ATP depletion and reductive stress of hypoxia (Lemasters et al., 1987). After addition of 2.5 mM NaCN and 20 mM 2-deoxyglucose, normal spontaneous contractions ceased after 1-2 minutes. After an average of 12 minutes, multiple blebs appeared on the myocyte surface which was followed quickly by hypercontraction into a rounded mass. Hypercontraction typically occurred in a time course of less than 30 seconds. After an average of 100 minutes, cell viability was lost as indicated by nuclear staining with propidium iodide.

Following reversal of chemical hypoxia by wash-out of the metabolic inhibitors, spontaneous contractions resumed after an average of 6 minutes in non-hypercontracted cells (Figure 9). However, after 10 minutes of hypercontraction, myocytes required an average of 32 minutes to resume spontaneous contractions upon removal of inhibitors. During this 32 minute period, the hypercontracted myocytes slowly returned to their pre-hypercontraction morphology. Viability of recovering hypercontracted and non-hypercontracted myocytes was maintained for at

least 48 hours. In these experiments ATP levels returned to 70% of control in both hypercontracted and non-hypercontracted cells after 10 minutes of wash-out of the metabolic inhibitors.

Intracellular pH During ATP Depletion

Chemical hypoxia produces an acidic intracellular pH which is protective against cell death (Gores et al., 1989a). Accordingly, one of our objectives was to determine if a similar phenomenon occurred in individual myocytes. During chemical hypoxia in myocytes, cytosolic pH decreased 0.5-0.8 units within 10 minutes and remained acidotic until close to the onset of cell death (Figure 10). Under these loading conditions, approximately 65% of the BCECF was inside the cytosolic compartment. The remainder was localized to mitochondria.

Protection by Acidic pH

To determine whether acidic pH was protective against the onset of cell death as reported for hepatocytes during chemical hypoxia (Gores et al., 1988; 1989a), loss of cell viability of purified myocytes exposed to anoxia was assessed at various values of extracellular pH. Anoxia was produced by infusion of submitochondrial particles whose respiration depleted ambient oxygen to less than 0.1 torr within 5 minutes (Herman et al., 1988). After 280 minutes of anoxia at pH 7.4, 92% of the myocyte nuclei had lost viability as indicated by propidium iodide labeling of myocyte nuclei (Figure 11). By contrast, cell killing was only 9-20% at pH 6.2-7.0.

DISCUSSION

One of our objectives was to evaluate long term viability and functional recovery of cultured neonatal cardiac myocytes after hypercontraction. Hypercontraction of hypoxic cardiac myocytes is presumed by most investigators to represent an irreversible step in the progression of cell injury even though cell death as assessed by uptake of trypan blue may not occur until much later. The presumption of irreversibility is based on the observation that contractile activity and relaxation are not observed quickly after reoxygenation as occurs when non-hypercontracted cells are reoxygenated. Here using reversible metabolic inhibitors, we demonstrated contractile recovery and long term viability in neonatal myocytes after reversal of 'chemical hypoxia', a model of metabolic inhibition with NaCN and 2-deoxyglucose which mimics the ATP depletion of anoxia. Neonatal cardiac myocytes have the advantage of spontaneous, synchronous contractions in culture which made them ideal for studying recovery of function as well as loss of viability.

Using the model of chemical hypoxia, we were able to maintain sterility and observe the cells over a 48 hour period. Individual myocytes exposed to chemical hypoxia ceased spontaneous contractions after 1-2 minutes, blebbed and hypercontracted after 12 minutes, and died after 100 minutes as defined by propidium iodide labeling of the nucleus. Those myocytes that recovered from chemical hypoxia before hypercontraction resumed spontaneous contractions after just 6 minutes. However, myocytes in hypercontraction for 10 minutes required about 30 minutes to resume regular spontaneous contractions. This 30 minute period of contractile dysfunction was not directly related to intracellular ATP concentration since recovery of ATP was the same in hypercontracted and non-hypercontracted myocytes. Taken together, these findings indicate that hypercontracture does not necessarily signify irreversible injury. Rather, hypercontraction may reflect a reorganization of the contractile apparatus.

Our working hypothesis is that the protracted period of contractile dysfunction observed in hypercontracted myocytes during recovery from chemical hypoxia may, in part, correspond to the phenomenon known as 'myocardial stunning' (Braunwald et al., 1982). Also known as post-ischemic dysfunction, myocardial stunning is defined as a mechanical dysfunction persisting after reperfusion of ischemic myocardium. The mechanism responsible for myocardial stunning has not been established but oxygen radical generation, ATP depletion, and perturbations in pH and Ca^{+2} homeostasis have been implicated (Bolli et al., 1988).

Another objective of this study was to determine if intracellular pH decreases in cardiac myocytes during ATP depletion and reduces the rate of anoxic cell killing. Intracellular acidosis occurred early during chemical hypoxia with pH decreasing 0.5-0.8 units in less than 10 minutes. In hepatocytes, this acidosis is protective against lethal cell injury (Gores et al., 1988). Thus, acidosis in myocytes may also protect myocytes against lethal hypoxic injury.

To test this hypothesis, we varied the extracellular pH between 6.2 to 7.4 and measured rates of anoxic cell killing of cardiac myocytes. At pH 7.4 cell killing was more than 90% after 280 minutes. By contrast, cell killing was reduced to 15% or less at acidotic pH (pH 6.2-7.0). Our data indicates, therefore, that acidosis is highly protective against lethal anoxic injury to myocytes. Thus, the naturally occurring tissue acidosis of ischemia which results from anaerobic glycolysis and ATP hydrolysis may be beneficial. Much attention has focused upon reperfusion injury to ischemic myocardium. Our failure to see aggravation of cell injury after reversal of chemical hypoxia suggests that changes of pH during reperfusion may be important in reperfusion injury. This interesting hypothesis is currently under investigation.

B. DIGITIZED VIDEO MICROSCOPY OF CALCIUM TRANSIENTS IN SPONTANEOUSLY CONTRACTING RAT NEONATAL MYOCYTES (with R.T. Inman, J.M. Bond, G.J. Gores and B. Herman)

INTRODUCTION

FURA-2 and related probes (see Grynkiewicz et al., 1985) are Ca^{2+}-sensitive fluorophores which have been employed to measure cytosolic free Ca^{2+} in single myocytes (see Wier et al., 1987 and Barry et al., 1987). For beating cells, spot measurement techniques are most often employed. These techniques yield values for the average cytosolic free Ca^{2+} of a single cell or small group of cells during the contractile cycle. With digitized video microscopy spatially resolved measurements of free Ca^{2+} are possible with a temporal resolution of 33 msec. Accordingly, the purpose of the present study was to assess the feasibility of employing digitized video microscopy to image and spatially resolve changes of free Ca^{2+} during the contractile cycle of single, spontaneously beating cardiac myocytes.

METHODS

Multiparameter Digitized Video Microscopy (MDVM)

The multiparameter digitized video microscope used for these studies consisted of a Zeiss IM-35 inverted microscope equipped with UV-transmitting optics and light source, an MTI-DAGE Model 66 intensified silicon-intensified target (ISIT) camera, a Sun 3/110 workstation containing a video analog to digital converter and frame memories from DataCube, imaging software from Inovision, a time lapse video casette recorder, and a Panasonic optical memory disk recorder (see DiGuiseppi et al., 1985; Lemasters et al., 1987). The high sensitivity of the ISIT camera allowed us to work at low levels of excitation energy and fluorophore concentration thus minimizing photobleaching and photodamage which might lead to disruption of normal cell activity. The ISIT camera was also used to obtain phase images. In some experiments, we loaded myocytes with more than one probe (i.e., FURA-2 and rhodamine 123). We sequentially examined emission from each fluorophore by changing excitation and emission filters under computer control.

Ratio Imaging

MDVM provides quantitative information regarding the amount of fluorophore emission. However, because MDVM provides a 2-dimensional image of a 3-dimensional object (i.e., the cell), FURA-2 fluorescence is proportional not only to free Ca^{2+} but also to cell thickness, regional FURA-2 concentration and dye leakage. To correct for these variables, images were acquired from cells at two different wavelengths, one which was Ca^{2+}-sensitive (340 nm) and another which was Ca^{2+}-insensitive (365 nm) or which changed in the opposite direction

(380 nm). By dividing values obtained at two wavelengths, ratios proportional to free Ca^{2+} were generated.

Measurement of Free Ca^{2+} Transients in Spontaneously Beating Rat Myocytes

Neonatal rat myocardial cells were isolated and cultured essentially as described by Harary and Farley (1963). After 3 days in culture, the cells were loaded with 4 μM FURA-2 acetoxymethyl ester for 30 minutes at 37°C in culture medium. Spontaneous contractions ceased during loading but resumed after another 90 minutes of incubation in culture medium without FURA-2 AM. Subsequently, coverslips containing myocytes were mounted on the stage of the MDVM system. After replacing culture medium with HEPES-buffered Krebs-Henseleit medium, myocytes were illuminated with 340, 365, and 380 nm light, and the fluorescence was imaged with an ISIT camera. In rhythmically contracting cells, images at 340, 365 and 380 nm were collected sequentially and stored at video rate during several contractions using an optical memory disk recorder. Subsequent to the experiment, the images were recalled, and total cellular fluorescence and fluorescence in 32x32 pixel boxes (10 μm^2) near the center and periphery of cells were determined in relation to the amount of contraction. Contraction was determined by measuring local displacement of the cell edges from a single reference image using a maximum-correlation registration algorithm. All data reduction was entirely automated.

RESULTS

Figure 12 illustrates actual fluorescence images during a contractile cycle. The sequence begins with cells in diastole (frame 11451). FURA-2 fluorescence increases abruptly in frame 11463, is slightly greater in frame 11467, and subsequently decreases slowly in frames 11471-11483 to the same level as frame 11451. Contraction is obvious in the real time playback of the video images although not readily discernible in the series of static images. The weakly labeled cells in the periphery whose fluorescence did not change during contraction were fibroblasts.

Fluorescence in single cells was integrated for each video frame in relation to the degree of shortening during the contractile cycle during consecutive sequences of contractions at the wavelengths 340, 365 and 380 nm. Using the beginning of contraction as a common reference, 340/380 nm fluorescence ratios (reflective of free Ca^{2+}) were calculated.

During the contractile cycle (1.3 sec), the 340/380 fluorescence ratio increased 1.8 fold (Figure 13). The rise occurred over 3-4 video frames (33 msec/frame) and was followed by a nearly linear decay over 17-19 frames. Contraction began at a point corresponding to 45% of the maximal increase of the fluorescence ratio. Relaxation began as the 340/380 fluorescence decreased to 30% of the maximal increase.

Fluorescence in 32x32 pixel boxes (10 μm^2) at the center and periphery of a beating myocyte was also digitized and ratioed for several contractile cycles in relation to the amount of contraction (Figure 14) The amplitude of changes of the 340/380 fluorescence ratio during contraction was greater at the cell periphery than at the cell center. Because the thickness of the cell decreased towards the periphery of the myocyte, absolute fluorescence was smaller at the periphery than the center (data not shown).

DISCUSSION

The present findings demonstrate that digitized video microscopy can quantitatively image cytosolic free Ca^{2+} in FURA-2-loaded myocytes with 10 μm^2 area resolution during the contractile cycle. As expected, contractions followed increases of cytosolic free Ca^{2+}. Contractions began about 100 msec after the beginning of the increase of 340/380 fluorescence at a point corresponding to 45% of the maximal increase. Similarly, relaxation began as 340/380 fluorescence decreased to 30% of its maximal increase.

The kinetic resolution of this approach is limited by the video frame rate to 33 msec. By using interlace defeat circuitry, 16 msec temporal resolution might be possible. However, the half signal detector lag time of the ISIT camera employed was only slightly less than 33 msec (Tsay et al., 1989). This limitation might be overcome by using an intensified video-rate CCD camera, now commercially available, which has a much shorter detector lag.

The amplitude of the changes of 340/380 fluorescence was greater at the periphery than at the center of myocytes which suggests that gradients of intracellular Ca^{2+} may develop during the contractile cycle. Such gradients might coordinate the timing and synchrony of sarcomere shortening within different parts of the cell for maximal mechanical and metabolic efficiency. However, more experiments are required to assure that the differences between the center and periphery of myocytes are not due to other factors. For example, experiments using rhodamine 123, a mitochondrial marker, and selective detergent extraction showed that approximately one-third of loaded FURA-2 was localized to mitochondria. Thus, regional differences of 340/380 fluorescence may represent regional differences of mitochondrial Ca^{2+}. In either case, further experiments are warranted to investigate this interesting phenomenon.

REFERENCES

Andersson BS, Aw TY, Jones DP (1987). Mitochondrial transmembrane potential and pH gradient during anoxia. Am J Physiol 252:C349-355.

Aw TY, Andersson BS, Jones DP (1987). Mitochondrial transmembrane ion distribution during anoxia. Am J Physiol 252:C356-C361.

Barry W, Peeters G, Rasmussen C.,Cunningham M. (1987) Role of changes in $[Ca^{2+}]_i$ in energy deprivation contracture. Circ Res 61:726-734.

Bellomo G, Orrenius S (1985). Altered thiol and calcium homeostasis in oxidative hepatocellular injury. Hepatology 5:876-882.

Bolli R, (1988). Oxygen-derived free radicals and postischemic myocardial dysfunction ('stunned myocardium'). J Am Coll Cardiol 12(1):239-249.

Bond JM, Gores GJ, Herman B, Lemasters JJ (1989). Reversal of hypercontraction, protection by acidic pH, and change of cytosolic pH during 'chemical hypoxia' and anoxia in cardiac myocytes. In "Video Microscopy, Herman B, Jacobson K (eds), in press.

Braunwald E, Kloner RA (1982). The stunned myocardium: prolonged, postischemic ventricular dysfunction. Circulation 66:1146-1149.

Bright GR, Fisher GW, Rogowska J, Taylor DL (1987). Fluorescence ratio imaging microscopy: temporal and spatial measurements of cytoplasmic pH. J Cell Biol 104:1019-1033.

DiGuiseppi J, Inman R, Ishihara A, Jacobson K, Herman B (1985). Applications of digitized fluorescence microscopy to problems in cell biology. BioTechniques 3:349-403.

Emaus RK, Grunwald R, Lemasters JJ (1986). Rhodamine 123 as a probe of transmembrane potential in isolated rat-liver mitochondria: spectral and metabolic properties. Biochim Biophys Acta 850:436-448.

Florine-Casteel K, Lemasters JJ, Herman B (1989). Digitized fluorescence polarization microscopy of DPH and related probes in cell-size vesicles composed of gel- or fluid-phase phospholipid. In "Video Microscopy", Herman B, Jacobson K, (eds), in press.

Gores GJ, Nieminen A-L, Fleishman E, Dawson TL, Herman B, Lemasters JJ (1988). Extracellular acidosis delays onset of cell death in ATP-depleted hepatocytes. Am J Physiol 255:C315-C322.

Gores GJ, Nieminen AL, Wray BE, Herman B, Lemasters JJ (1989a) Intracellular pH during 'chemical hypoxia' in cultured rat hepatocytes. J Clin Invest 83:386-396.

Gores GJ, Flarsheim CE, Dawson TL, Nieminen A-L, Herman B, Lemasters JJ (1989b). Swelling, reductive stress, and cell death during chemical hypoxia in hepatocytes. Am J Physiol 257:C347-C354.

Grynkiewicz G, Poenie M, Tsien R (1985). A new generation of Ca^{2+} indicators with greatly improved fluorescence properties. J Biol Chem 260:3440-3450.

Harary I, Farley B (1963). In vitro studies in single cell beating rat heart cells I. Growth organization. Exp Cell Res 29:451-465.

Harootunian A, Eckert B, Minta A, Tsien RY (1988). Ratio imaging using the newly developed fluorescent sodium indicators in rat embryo fibroblasts. FASEB J 2:A728.

Lemasters JJ, Stemkowski CJ, Ji S, Thurman RG (1983). Cell surface changes and enzyme release during hypoxia and reoxygenation in the isolated, perfused rat liver. J Cell Biol 97:778-786.

Lemasters JJ, DiGuiseppi J, Nieminen A-L, Herman B, (1987). Blebbing, free Ca^{2+} and mitochondrial membrane potential preceding cell death in hepatocytes. Nature 325:78-81.

Nieminen A-L, Gores GJ, Wray BE, Tanaka Y, Herman B, Lemasters JJ (1988). Calcium dependence of bleb formation and cell death in hepatocytes. Cell Calcium 9:237-246.

Tsay T-T, Inman R, Wray BE, Herman B, Jacobson K (1989) Characterization of low light level video cameras for fluorescence microscopy. In "Video Microscopy", Herman B, Jacobson K (eds), in press.

Tsien R (1989). Fluorescent indicators of ion concentrations. Meth Cell Biol 30:127-156.

Ulrich R, Elliget KA, Rosnick DK (1989). Purification of neonatal rat cardiac cells by centrifugal elutriation. J Tiss Cult Meth 11:217-221.

Wier WG, Cannell MB, Berlin JR, Marban E, Lederer WJ (1987). Cellular and subcellular heterogeneity of $[Ca^{2+}]_i$ in single heart cells revealed by Fura-2. Science 235:325-328.

Table 1. *Fluorescent Probes of Cell Function*

PROBE	EXCITATION WAVELENGTH (nm)	EMISSION WAVELENGTH (nm)	RESPONSE OF FLUORESCENCE
Fura-2	340	>450	Ca^{2+}-dependent, increases with increasing Ca^{2+}
	362	>450	Ca^{2+}-independent
	380	>450	Ca^{2+}-dependent, decreases with increasing Ca^{2+}
Rhodamine 123	490	>530	Proportional to mitochondrial membrane potential
Propidium iodide	546	>590	Labels nuclei of nonviable cells (analogous to trypan blue)
Acridine orange	365	>600	Labels lysosomes (punctate orange)
	490	530-560	Labels RNA and DNA (diffuse green)
	546	>590	Labels lysosomes (punctate red)
Fluorescein-dextran	490	>530	Labels lysosomes, responds to lysosomal pH
Fluorescein diacetate	490	>530	Diffuse fluorescence retained by living cells
BCECF	490	>530	pH-dependent, increases with increasing pH
	440	>530	pH-independent
Rhodamine-dextran	546	>590	Labels lysosomes
Rhodamine microspheres	546	>590	Labels prelysosomal endocytic compartment
Monobromobimane	380	>470	Labels protein and non-protein thiols
Monochlorobimane	380	>470	Labels non-protein thiols (glutathione)
Dichlorofluoroscin	490	>530	Lipid peroxides, activated oxygen species
SBFI	340	>450	Increases with increasing Na^+
	380	>450	Decreases with increasing Na^+
Trimethylammonium diphenylhexatriene (TMA-DPH)	365	>420	Labels plasma membrane, fluid regions quenched by TEMPO

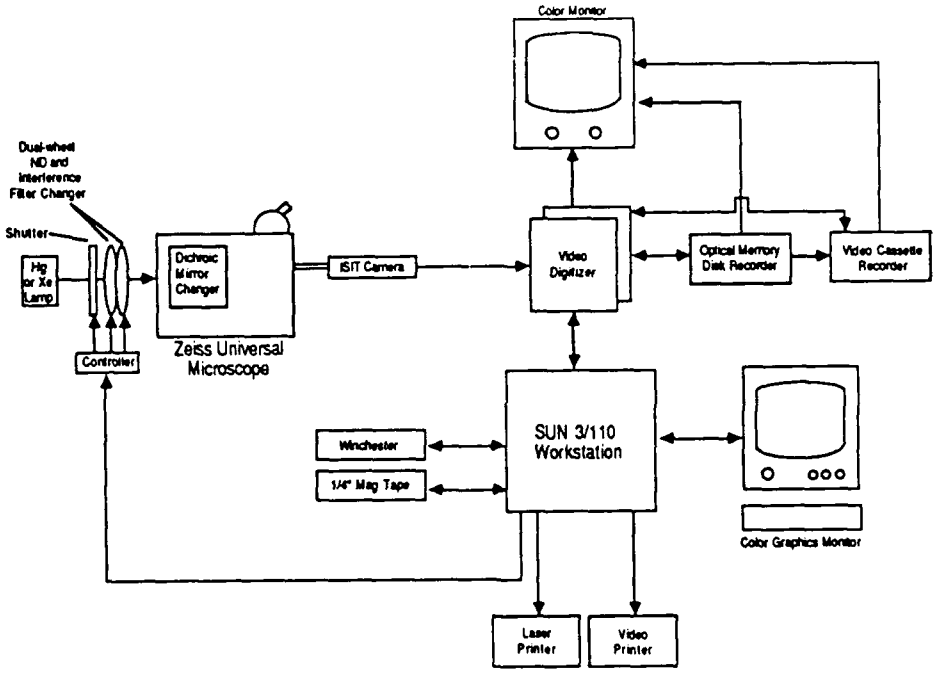

Figure 1. Schematic of the multiparameter digitized video microscope system.

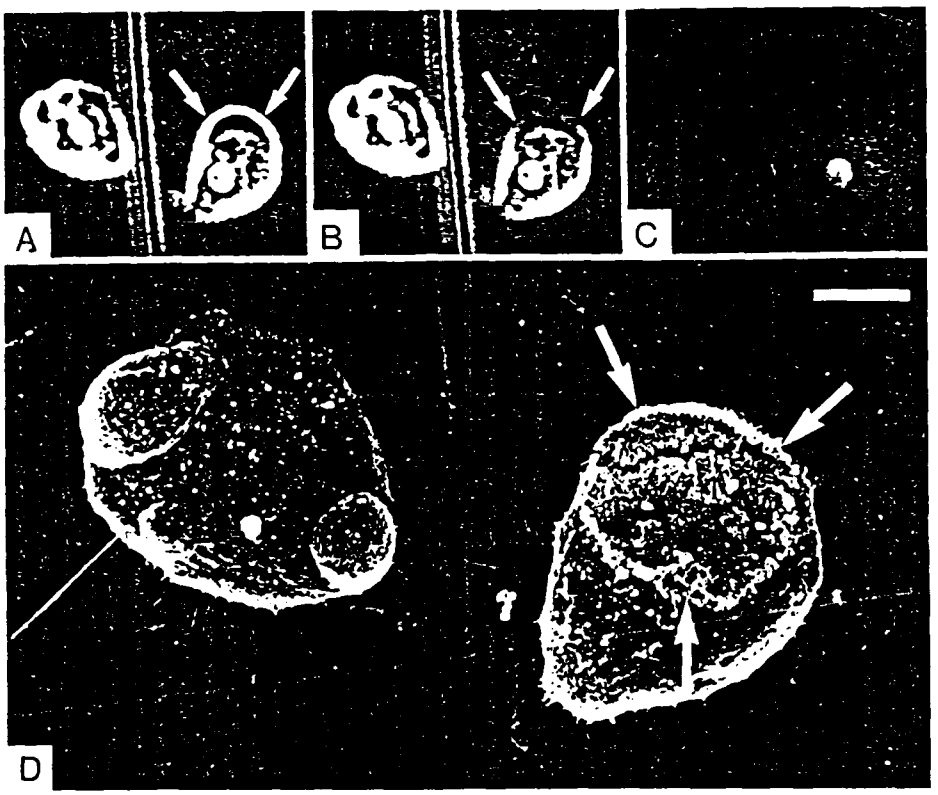

Figure 2. Plasma membrane changes during bleb rupture - After about 65 minutes of chemical hypoxia with 5 mM KCN and 10 mM iodoacetate, terminal blebs had formed on two cells (panel A). After 200 msec (1 video frame in the time-lapse recording), the terminal bleb on the cell to the right had ruptured (panel B) allowing labeling with propidium iodide several seconds later (panel C). The coverslip was then flooded with fixative and prepared for scanning electron microscopy (panel D). A large surface discontinuity (arrows) bordered by small membrane vesicles formed at the point of bleb rupture. The surface of the cell to the left which continues to exclude propidium iodide is smooth and continuous. Bar is 10 μm.

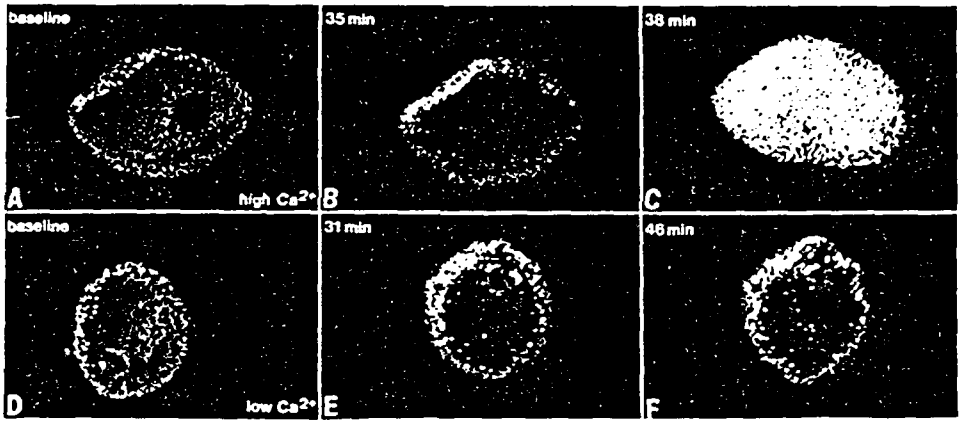

Figure 3. Distribution of cytosolic free Ca^{2+} in single cultured hepatocytes - FURA-2-loaded hepatocytes in high Ca^{2+} (1.27 mM) (panels A-C) or low Ca^{2+} ($\approx$2 μM) (panels D-F) medium were exposed to 2.5 mM KCN plus 0.5 mM iodoacetate. Blebs were well developed after 30 minutes of chemical hypoxia in both low and high Ca^{2+} media, although the surface blebs are not well seen in these pseudocolored images. Note the marked increase of free Ca^{2+} between 35 minutes (panel B) and 38 minutes (panel C) in high Ca^{2+} medium. After longer than 38 minutes, cell viability was lost and images could no longer be obtained because of Fura-2 leakage from the cell. For the hepatocyte in low Ca^{2+} medium, viability was lost shortly after 46 minutes of exposure to the metabolic inhibitors. Free Ca^{2+} did not increase prior to cell killing (panels E and F). Colors represent ranges of cytosolic free Ca^{2+} concentrations: blue, <100 nM; green, 100-250 nM; yellow, >250 nM. Crescents of yellow and blue in some images are stage movement artifacts.

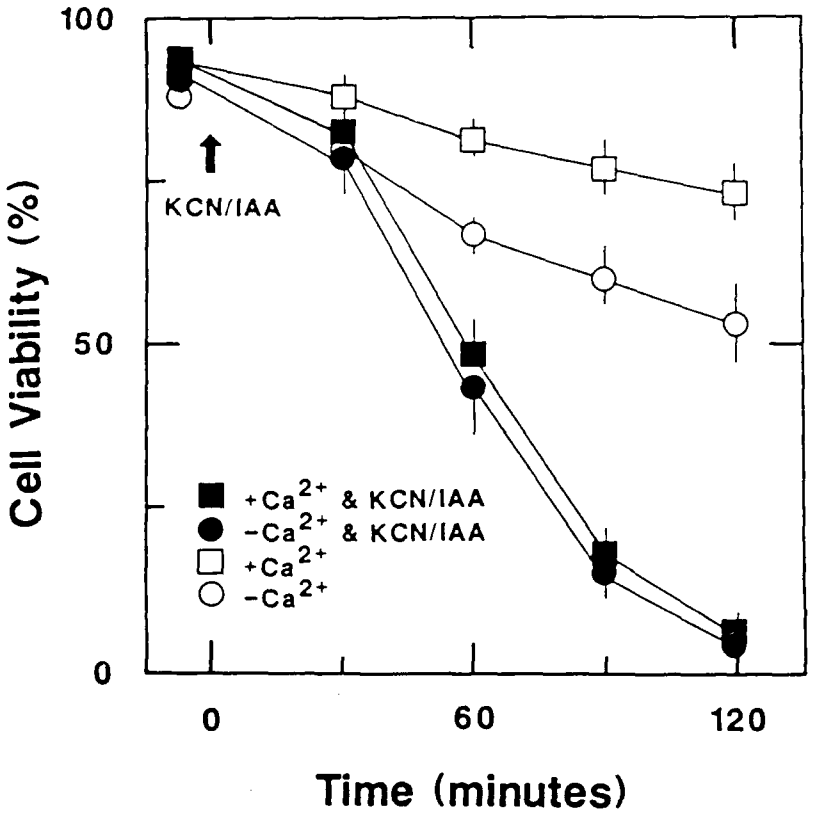

Figure 4. Cell viability during chemical hypoxia in high and low Ca^{2+} media - Viability of freshly isolated hepatocytes (100,000/ml) was assessed by propidium iodide fluorometry (Gores et al., 1988) after chemical hypoxia with 2.5 mM KCN and 0.5 mM iodoacetate. Rates of cell killing were virtually identical in high and low Ca^{2+} media.

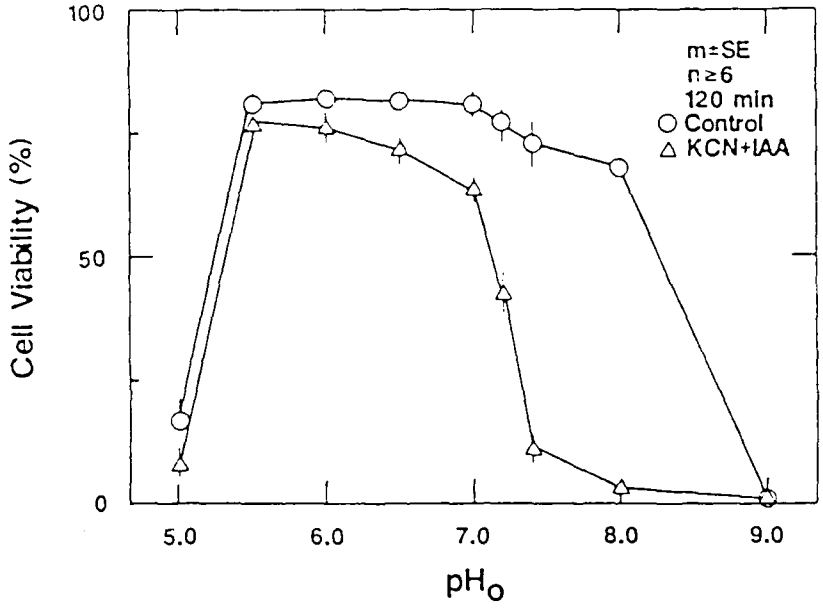

Figure 5. Protection by acidosis against cell killing during chemical hypoxia - Extracellular pH (pH_o) was changed simultaneously with the addition of 2.5 mM KCN and 0.5 mM iodoacetate. Control hepatocytes were incubated without metabolic inhibitors. Cell viability was assessed by propidium iodide fluorometry after 120 minutes.

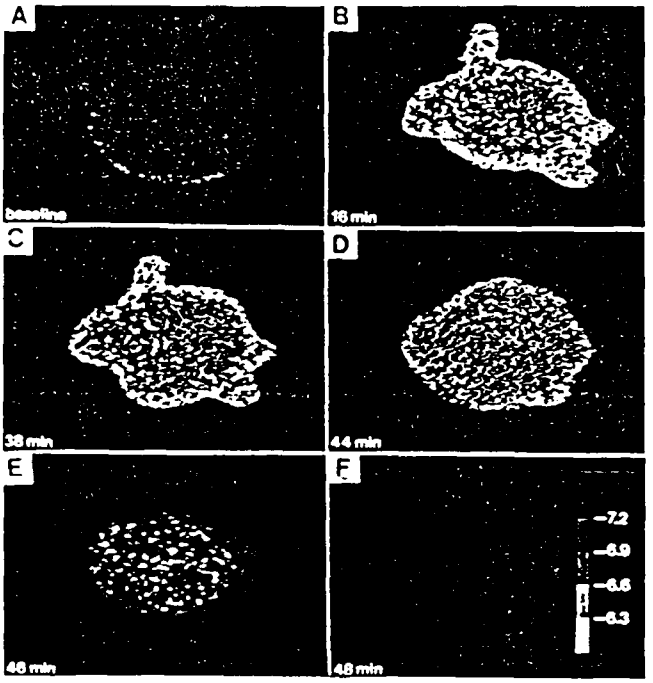

Figure 6. Intracellular pH during chemical hypoxia - Intracellular pH of a 1-day cultured hepatocyte was measured by BCECF ratio imaging after various times of exposure to KCN and iodoacetate. Note intracellular acidosis after addition of metabolic inhibitors (panels B-D). pH rose sharply after 46 minutes (panel E). At the same time BCECF was beginning to escape as evidenced by erosion of the image. After 48 minutes, viability was lost (panel F).

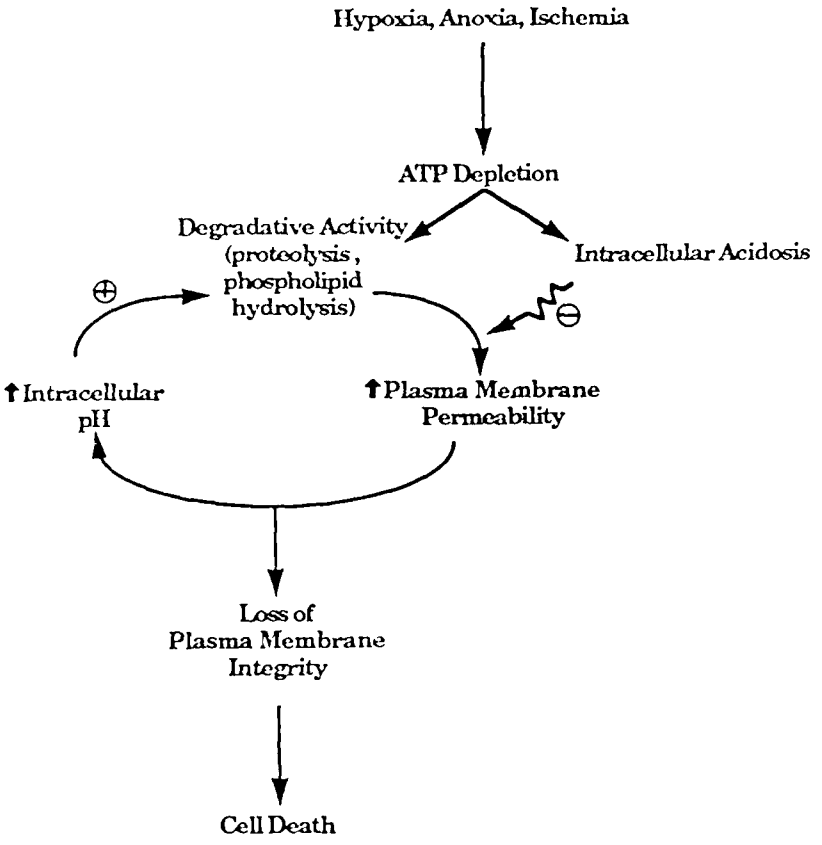

Figure 7. Intracellular pH and hypoxic injury - In this hypothetical scheme, ATP depletion and anaerobic glycolysis during anoxic and ischemic stress lead to intracellular acidosis and activation of proteases and phospholipases. Intracellular acidosis protects against loss of viability by inhibiting the activated enzymes. Ultimately, action by the degradative enzymes leads to proton leakage through the membrane causing a vicious cycle of increasing intracellular pH and accelerating degradative activity which culminates rapidly in cell death.

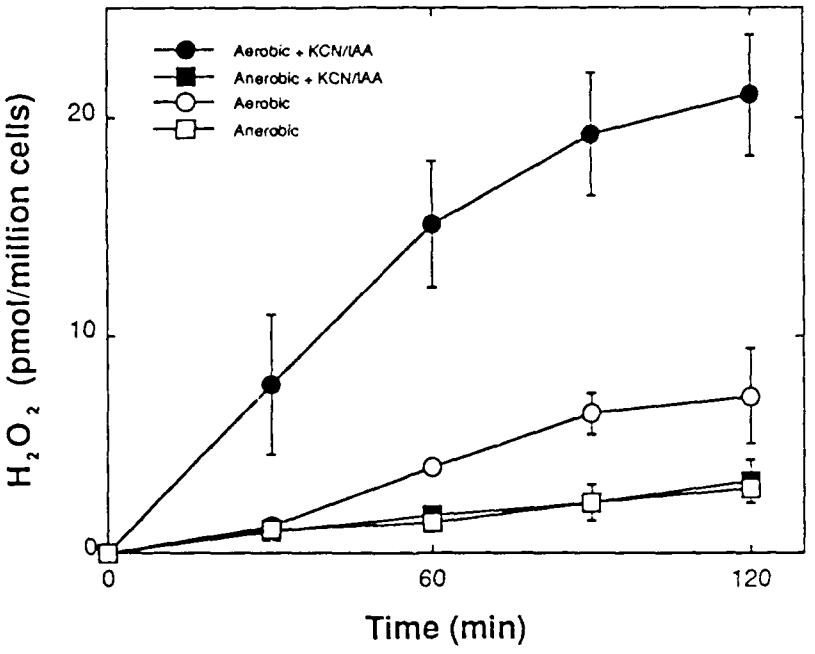

Figure 8. Hydroperoxide generation during chemical hypoxia - Hepatocytes loaded with dichlorofluorescin were incubated in aerobic or anaerobic buffer in the presence or absence of KCN plus iodoacetate (KCN/IAA). Hydroperoxide formation as indicated by dichlorofluorescein fluorescence was accelerated during chemical hypoxia in aerobic medium.

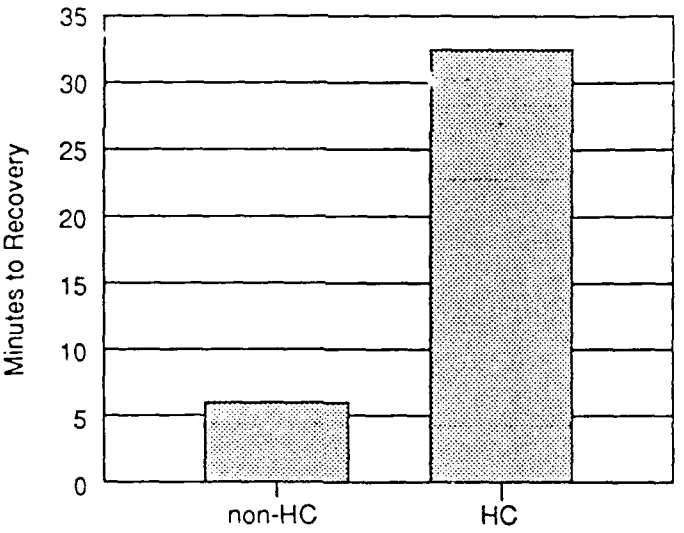

Figure 9. Minutes to resumption of spontaneous contractions in non-hypercontracted myocytes (non-HC) and hypercontracted myocytes (HC) after reversal of chemical hypoxia - Cultures of purified myocytes in 35 mm culture dishes were exposed to 2.5 mM NaCN and 20 mM 2-deoxyglucose for either 10 minutes or the time to hypercontraction plus 10 minutes (average total hypoxic time was 22 minutes). Reversal of metabolic inhibition was accomplished by exchange with fresh medium.

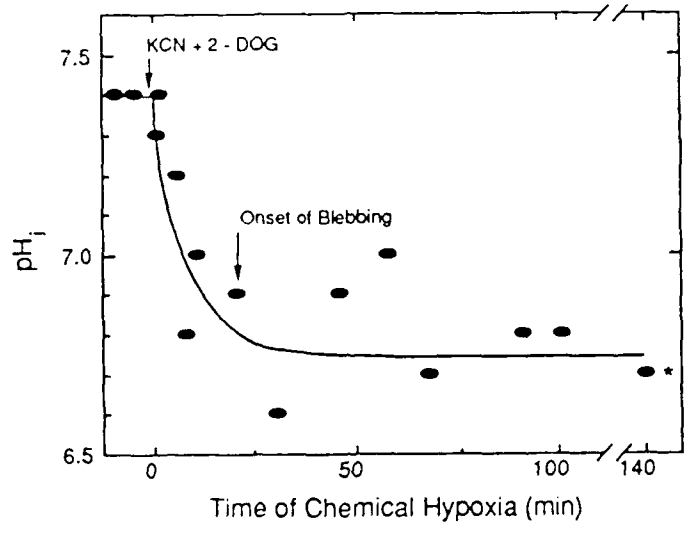

Figure 10. Intracellular pH of a single cultured myocyte during ATP depletion by chemical hypoxia - A 4-day old non-purified myocyte on a glass coverslip was incubated with 5 μM BCECF-acetoxymethyl ester for 30 minutes at 37°C. Intracellular pH was calculated by ratio imaging of BCECF fluorescence using MDVM after addition of 2.5 mM NaCN and 20 mM 2-deoxyglucose. Asterisk indicates loss of cell viability.

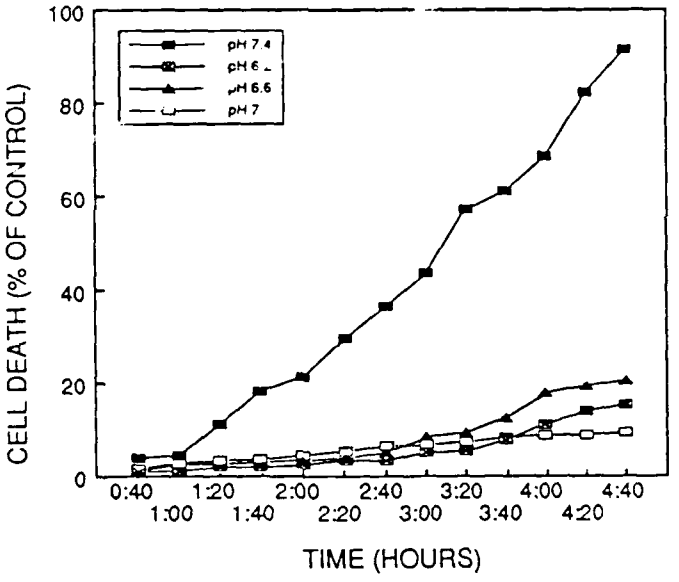

Figure 11. Protection against anoxic killing by an acidic extracellular pH - Purified cultures of 5-day old myocytes on polystyrene coverslips were mounted in a gas-tight chamber. Anoxia was created by infusion of 1 mg/ml submitochondrial particles, 5 mM succinate, and 20 mM 2-deoxyglucose. Losse of cell viability was determined by propidium iodide staining of myocyte nuclei over time

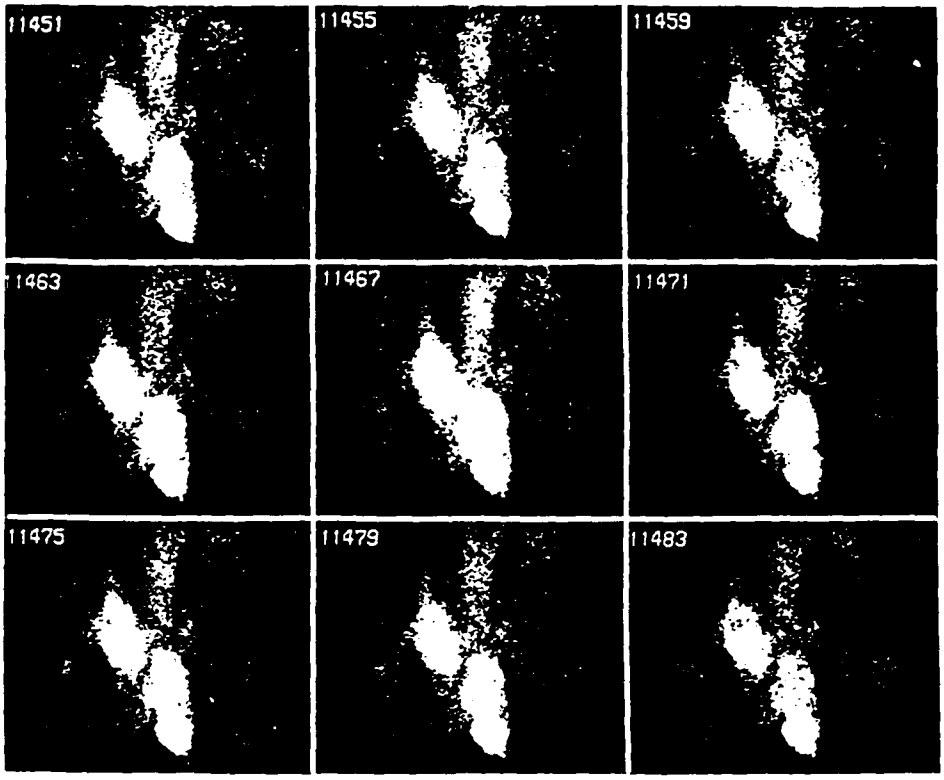

Figure 12. Fluorescence images of calcium transients in spontaneously contracting neonatal myocytes - Ca^{2+} dependent fluorescence at 340 nm was recorded in spontaneously contracting three-day cultured myocytes loaded with FURA-2. Displayed is every fourth video frame during a single contractile cycle from a small group of synchronously beating cells.

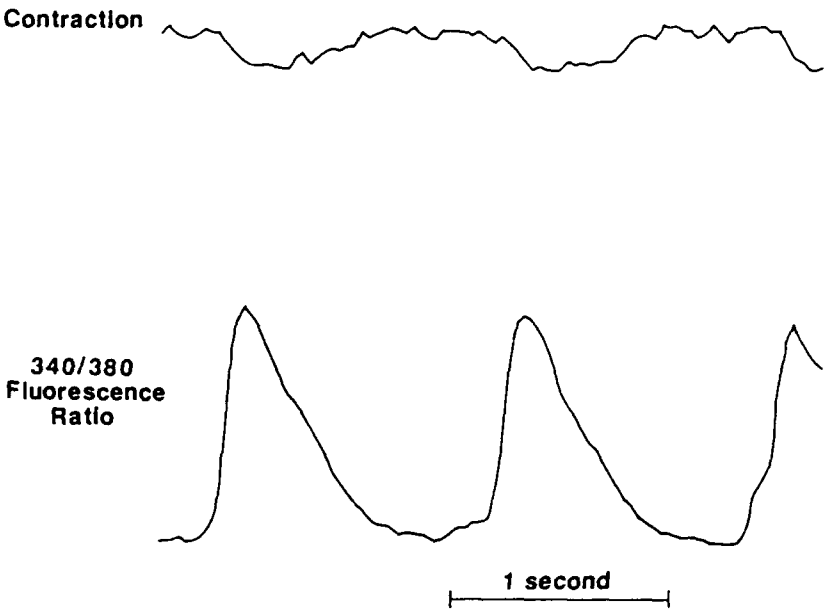

Figure 13. $\underline{Ca^{2+}}$ <u>transients in a single spontaneously contracting rat neonatal myocyte</u> - Three day cultured rat neonatal myocytes were loaded with FURA-2. In a single rhythmically contracting cell, fluorescence images at 340 nm and then at 380 were recorded during several contractions using an optical memory disk recorder. Single frames were played back, digitized, ratioed, and averaged for the entire cell to generate 340/380 fluorescence ratios, a measurement which is proportional to free Ca^{2+}. Cell contraction was determined from length changes of the fluorescence images.

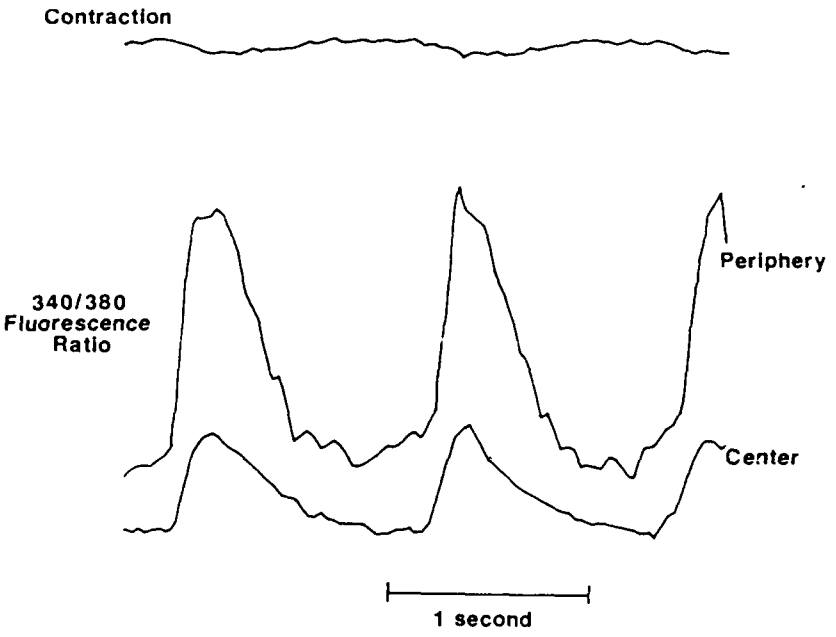

Figure 14. $\underline{Ca^{2+}}$ <u>transients in 10μm^2 areas at the center and periphery of a spontaneously contracting rat neonatal myocyte</u>. 340/380 fluorescence ratios were calculated in 32x32 pixel boxes at the center and periphery of a single spontaneously beating myocytes.

DISTRIBUTION LIST

Cell Biology of Trauma Program

Annual, Final and Technical Reports (one copy each)

INVESTIGATORS

Dr. Michael Artman
Dept. of Pediatrics
Univ. of South Alabama
Medical Center
2451 Fillingim Street
Mobil, AL 36617

Dr. Margaret S. Burns
Dept. of Ophthalmology
Univ. of California, Davis
1603 Alhambra Boulevard
Sacramento, CA 95816

Dr. Robert J. Cohen
Dept. of Biochemistry and
Molecular Biology
College of Medicine
Box J-245, JHMHC
University of Florida
Gainesville, FL 32610

Dr. Dipak K. Das
Department of Surgery
Univ. of Connecticut
Health Center
Farmington, CT 06032

Dr. Thomas M. Devlin
Chairman, Dept. of Biological Chemistry
Hahnemann University
230 Broad Street
Philadelphia, PA 19102

Dr. Marvin A. Karasek
Dept. of Dermatology
Stanford University School of Medicine
Stanford, CA 94305

Dr. John J. Lemasters
Dept. of Cell Biology and Anatomy
School of Medicine
University of North Carolina
Campus Box 7090
Chapel Hill, NC 27599

Dr. Alfred H. Merrill, Jr.
Dept. of Biochemistry
Emory University School
of Medicine
Atlanta, GA 30322

LCDR Douglas H. Robinson
Diving Medicine Dept.
Naval Medical Research Inst.
NMC NCR
Bethesda, MD 20814-5055

Dr. Benjamin F. Trump
Dept. of Pathology
Univ. of Maryland
School of Medicine
Baltimore, MD 21201

Annual, Final and Technical Reports (one copy each except as noted)

ADMINISTRATORS

Dr. Jeannine A. Majde, Code 1141SB
Office of Naval Research
800 N. Quincy Street
Arlington, VA 22217-5000

Program Manager, Code 1213
Human Factors/Biosciences Division
Office of Naval Research
800 N. Quincy Street
Arlington, VA 22217-5000

Administrator (2 copies) (Enclose DTIC Form 50)
Defense Technical Information Center
Building 5, Cameron Station
Alexandria, VA 22314

Program Manager, Code 223
Support Technology Directorate
Office of Naval Technology
800 N. Quincy Street
Arlington, VA 22217-5000

Administrative Contracting Officer
ONR Resident Representative
(address varies - obtain from business office)

Annual and Final Reports Only (one copy each)

DoD ACTIVITIES

Commanding Officer
Naval Medical Center
Washington, DC 20372

Directorate of Life Sciences
Air Force Office of Scientific Research
Bolling Air Force Base
Washington, DC 20332

Commanding Officer
Naval Medical Research & Development Command
National Naval Medical Center
Bethesda, MD 20814

Library
Armed Forces Radiation Research Institute
Bethesda, MD 20814-5145

Library
Naval Medical Research Institute
National Naval Medical Center
Bethesda, MD 20814

Commander
Chemical and Biological Sciences Division
Army Research Office, P.O. Box 12211
Research Triangle Park, NC 27709

Commander
U.S. Army Research and Development Command
Attn: SGRD-PLA
Fort Detrick
Frederick, MD 21701